

Manipulated Slow Release of Florfenicol Hydrogels for Effective Treatment of Anti-Intestinal Bacterial Infections

Wanhe Luo^{1,2}, Mengdi Zhang¹, Yongtao Jiang¹, Guocai Ma³, Jinhuan Liu^{1,4}, Ali Sobhy Dawood⁵, Shuyu Xie⁶, Samah Attia Algharib⁷

¹College of Animal Science and Technology, Tarim University, Alar, Xinjiang, 843300, People's Republic of China; ²Key Laboratory of Livestock and Forage Resources Utilization Around Tarim, Ministry of Agriculture and Rural Areas, Tarim University, Alar, Xinjiang, 843300, People's Republic of China; ³Instrumental Analysis Center, Tarim University, Alar, Xinjiang, 843300, People's Republic of China; ⁴Lab for Sustainable Antimicrobials, Department of Pharmacy, Sichuan Agricultural University, Chengdu, Sichuan, 610000, People's Republic of China; ⁵Medicine and Infectious Diseases Department, Faculty of Veterinary Medicine, University of Sadat City, Sadat city, 32897, Egypt; ⁶National Reference Laboratory of Veterinary Drug Residues (HZAU) and MARA Key Laboratory for Detection of Veterinary Drug Residues, Huazhong Agricultural University, Wuhan, Hubei, 430070, People's Republic of China; ⁷Department of Clinical Pathology, Faculty of Veterinary Medicine, Benha University, Moshtohor, Toukh, 13736, Egypt

Correspondence: Wanhe Luo; Samah Attia Algharib, Email luowanhe0728@163.com; samah.alghareeb@fvtm.bu.edu.eg

Objective: The difficulty of establishing slow release at intestinal infection sites, weak antibacterial effects, as well as the limited broad use of florfenicol oral formulations are the main targets of the current study. Novel hydrogels derived from sodium alginate were developed using a complexation form for florfenicol delivery to achieve slow release at the site of intestinal infection and enhance its antibacterial activity against *Escherichia coli*.

Methods: The optimal formulation, physicochemical properties, stability, pH-responsive performance, antibacterial activity, and in vitro biosafety of the florfenicol hydrogels have been studied systematically.

Results: The created hydrogels had a consistent spherical morphology, with an average diameter of 531.9 ± 12.6 nm. Energy dispersive spectroscopy and Fourier transform infrared indicated that florfenicol hydrogels have been successfully prepared through complexation force. Furthermore, it is shown that florfenicol hydrogels hold outstanding stability, excellent sustained release, and faster swelling and release at intestinal pH due to pH-responsiveness. The florfenicol hydrogels had no obvious structural destruction in simulated gastric juice (pH=1.2) for 12 hrs and were highly stable. However, the hydrogels began to be destroyed after 5 minutes in simulated intestinal fluid (SIF), and this decomposition was continuous. With the decomposition of the structure of florfenicol hydrogels, the encapsulated florfenicol was also slowly released, and thus, it achieves the slow-release effect. Additionally, the florfenicol hydrogels showed a low hemolytic ratio and greater antibacterial activity compared with florfenicol.

Conclusion: The blended formulation creates a promising oral matrix intended for the slow-release of florfenicol along the gastrointestinal tract.

Keywords: florfenicol, intestinal bacterial infections, hydrogels, sodium alginate, slow-release

Introduction

The treatment of numerous ailments in farm and aquatic animals is the primary use of bacteriostatic antibiotics such as florfenicol in veterinary medicine. By preventing ribosomal activity, which interferes with bacterial protein synthesis, this synthetic counterpart of chloramphenicol and thiamphenicol has been demonstrated to be effective against a variety of Gram-positive and Gram-negative bacterial species.¹ Furthermore, it has been discovered that florfenicol has anti-inflammatory qualities and inhibits the growth of immune cells and the production of cytokines.² Florfenicol is commonly used in veterinary clinics due to its good pharmacodynamics and pharmacokinetics, such as wide distribution in vivo, long half-life, and long-term maintenance of effective blood drug concentration.³ As one of the animal-specific antibiotics, florfenicol has excellent antibacterial activity against various Gram-positive, Gram-negative bacteria, and

mycoplasma. It has a potent effect against *Haemophilus*, *Shigella*, *Salmonella*, *Escherichia coli*, *Pneumococcus*, *Influenza bacilli*, *Streptococcus*, *Staphylococcus aureus*, *Chlamydia*, *Leptospira*, and *Rickettsia*.^{4–6} Oral dosing is the best option for treating animal intestinal bacterial pathogens.⁷ Premix florfenicol is used to treat pleurisy pneumonia and atrophic rhinitis, as well as necrotizing enteritis in pigs, and its water-soluble formula is commonly used to control diseases in poultry.^{1,4} Florfenicol is rapidly absorbed in the intestinal tract, resulting in weak antibacterial actions.⁸ Therefore, oral formulations of florfenicol have limited use in veterinary clinics. Thus, achieving slow release at intestinal infection locations while enhancing its antibacterial activity is a significant challenge.

Hydrogels, a revolutionary drug delivery technology, are three-dimensional hydrophilic networks made of flexible polymer chains that swell when exposed to water or biological fluids.^{9–11} They can hold a lot of fluid while retaining their three-dimensional structure, and they can be shaped into almost any shape or form. Natural hydrogels, such as alginate, collagen, fibrin, hyaluronic acid, chitosan, agarose, or starch, and synthetic hydrogels, such as poly (ethylene glycol), poly(vinyl alcohol), or polymethyl methacrylate, are the two categories of hydrogels. Natural hydrogels have strong bioaffinity and biocompatibility, despite some disadvantages related to their variable composition and inadequate processing reproducibly.¹² Hydrogels can protect antimicrobial agents from being degraded by gastric acid after being encapsulated by hydrogel materials, achieve slow release at the site of intestinal infection, and enhance antibacterial activity against intestinal bacteria.¹³ For example, encapsulated colistin with hyaluronic acid (HA), D-mannosamine hydrochloride (DMH), and carboxymethyl cellulose efficiently inhibits gastric acid decomposition, mucus clearance, and intestinal epithelial impermeability, thus enhancing the antibacterial activity of colistin against intestinal bacteria.¹⁴ Xu et al prepared composite nanosystems of polylactic acid folate and chitosan for oral delivery of insulin, resulting in a significantly higher oral bioavailability (7.22%) compared to insulin alone (0.51%).¹⁵ In addition, sodium alginate (SA), as a natural polysaccharide polymer material, is widely used to encapsulate antimicrobial agents, avoid drug degradation by gastric acid, achieve targeted release at intestinal infection sites, and enhance the obtained antibacterial activity.^{16–18} SA hydrogels had pH-responsive performance and had no obvious change in the acidic medium, but they will rapidly swell and become larger at pH=7.0. This property allows SA hydrogels to avoid destruction by gastric acid and rapidly swell in the intestine to release drugs and achieve the goal of targeted release.⁵ In addition, SA hydrogels, as hemostatic agents, are used as hemostatic sponges, hemostatic gauzes, hemostatic films, scald gauzes, spray hemostatic agents, etc.¹⁹ The hemostatic property makes SA hydrogels applicable to bleeding caused by intestinal bacteria. It is reported that SA can form stable hydrogels after complexing with Ca^{2+} . Tilmicosin encapsulated by the complexation of SA and Ca^{2+} had ideal physicochemical properties and was used to treat mastitis caused by *Staphylococcus aureus*.²⁰

In view of this, florfenicol was encapsulated by the complexation force of SA and Ca^{2+} to form florfenicol hydrogels in order to achieve the effect of slow release and enhance its antibacterial activity against intestinal bacteria. The optimal formulation, physicochemical properties, stability, pH-responsive performance, antibacterial activity, and in vitro bio-safety have been studied systematically. The aim of this work is to enhance the antibacterial activity of florfenicol against *E. coli* and provide reference data for the treatment of bacterial enteritis by slowly releasing florfenicol encapsulated by the complexation of SA and Ca^{2+} .

Materials and Methods

Florfenicol (98.0%), SA, and calcium chloride (CaCl_2) were supplied by Macklin (China). Phosphate-buffered saline (PBS), tryptic soy broth (TSB), and physiological saline were purchased from “Dingyuan Co., Ltd. (China)”. *E. coli* ATCC 25922 and *E. coli* isolates were provided by the “Tarim University Engineering Laboratory for Tarim Animal Diseases Diagnosis and Control (China)”. The water was prepared using a Milli-Q system (Millipore, USA). The remaining reagents in the text were analytical grade or of equal quality.

Formulation of Florfenicol Hydrogels

Florfenicol hydrogels were prepared through the complexation between SA and Ca^{2+} . In short, SA (150, 250, and 350 mg) and CaCl_2 (2.5, 5.0, and 7.5 mg) were dissolved in 10 and 1 mL ultrapure water, respectively, to obtain different concentrations of SA hydrogels (15, 25, and 35 mg/mL) and Ca^{2+} solutions (2.5, 5.0, and 7.5 mg/mL), respectively. Meanwhile, 0.2 g of florfenicol was dissolved in 2 mL of N,N-dimethylformamide to form florfenicol solution.

Subsequently, the Ca^{2+} solution and the florfenicol solution were mixed to obtain a florfenicol@ Ca^{2+} mixed solution for 1 h. Finally, a florfenicol@ Ca^{2+} mixed solution was dropped into the SA hydrogels to obtain florfenicol hydrogels at 1000 RPM. Correspondingly, Ca^{2+} solution was dropped into SA hydrogels to form blank hydrogels at 1000 RPM. The florfenicol hydrogels with different formulas were placed in a bottle, and their gelling properties were observed at 0° , 45° , 90° , and 180° to choose the optimal formula.

Optimization of Formula Using Box-Behnken Response Surface Analysis

In this study, the Design-Expert 8.0 software “State-Ease, Inc., Minneapolis, MN, USA” yielded exact results for the perfect SA and CaCl_2 concentrations as well as the ideal speed. The ideal concentrations of SA and CaCl_2 , as well as the optimal speed were found using the loading capacity (LC) and encapsulation efficiency (EE). The variables and levels of the Box-Behnken design are shown in Table 1. For each sample, three formulations were created. The mean \pm SD is used to express the data.

Physical Characteristics of Florfenicol Hydrogels

The Electron Microscopy

The appearance, transmission electron microscopy “TEM, JEM-2100Plus, Japan”, scanning electron microscopy “SEM, APREOS, Thermo Scientific Inc., USA”, and resolvability of optimal florfenicol hydrogels were systematically evaluated. In brief, the fresh florfenicol hydrogels were placed in a bottle, and their gel properties were observed at 0° , 45° , 90° , and 180° . Simultaneously, the morphology of fresh florfenicol hydrogels was observed by TEM, and the elemental analysis was determined by energy-dispersive spectroscopy “EDS; X-Max N 150, Oxford, UK”. Subsequently, the fresh florfenicol hydrogels were freeze-dried by the lyophilizer “FDU-1200, Shanghai Lingyi Biotechnology Co., Ltd., Japan”, and their morphology was observed by SEM. Finally, the freeze-dried florfenicol hydrogels were dissolved in ultrapure water again to evaluate their resolvability.

The Mean Size, Zeta Potential (ZP), and Polydispersity Index (PDI)

The mean size, ZP, and PDI of florfenicol hydrogels were measured using the “Zetasizer ZX3600 (Malvern Instruments, UK)” following the 100-fold dilution and 30-minute ultrasonic cleaning by “an ultrasonic cleaner (BILON3-120A, China)”. Three examinations were conducted on the samples, and the mean \pm SD of the results was reported.

Table 1 Single-Factor Experimental Design and Values of the Responses for Florfenicol Hydrogels

Run	SA (mg/mL)	CaCl_2 (mg/mL)	LC (%)	EE (%)
1	25	2.5	12.1	71.3
2	25	5	10.9	65.3
3	25	5	10.9	65.3
4	25	5	10.9	65.3
5	15	7.5	7.4	33.9
6	15	2.5	11.6	48.6
7	35	2.5	12.7	90.4
8	25	7.5	9.8	52.3
9	25	5	10.9	65.3
10	35	5	12.4	90.4
11	25	5	10.9	65.3
12	35	7.5	13	89.9
13	15	5	9.7	41.1

Fourier Transform Infrared (FTIR)

After the florfenicol hydrogels were freeze-dried, the FTIR of SA, florfenicol, and florfenicol hydrogels were analyzed using an FTIR spectrophotometer “Nicolet iS50, Thermo Scientific Inc., USA”. In summary, the dried samples that had been finely pulverized were placed onto the disk. Carson apodization was used to scan each disk 32 times at 2 mm/size and 4 cm^{-1} of resolution.

Rheological Analysis

Using a parallel plate (P20 TiL), rheological measurements of florfenicol hydrogels were performed using a HAAKE MARS RS6000 rheometer (Thermo Scientific, Germany). The florfenicol hydrogels were put on a level plate, and silicone oil was used to seal the parallel plate's edges. Using a temporal sweep test, the hydrogels' storage modulus (G') and loss modulus (G'') were determined.

Adhesiveness

After the florfenicol hydrogels were placed at the bent fingers, the adhesiveness of the florfenicol nanogels was evaluated by the state of the joint at different angles (0° , 45° , 90° , and 180°).

Stability Evaluation

The durability of florfenicol hydrogels was evaluated using influencing-factor studies, which comprised high temperature (40°C), high humidity ($90\%\pm 5\%$), and bright light ($4500\pm 500\text{ L}\times$). For the high-temperature test, the florfenicol hydrogels were placed in a container and incubated for 10 days at 40°C , $90\%\pm 5\%$ for the humidity test, and $4500\pm 500\text{ L}\times$ for illumination. Samples were obtained on the fifth and tenth days to assess the variations in their appearance, mean size, ZP, PDI, UV-vis spectrophotometry, FTIR spectrophotometer, LC, and EE.

pH-Responsive Performances of Florfenicol Hydrogels

In this study, “simulated gastric juice (SGJ) and simulated intestinal fluid (SIF)” were prepared to evaluate the pH-responsive performance of florfenicol hydrogels in the gastrointestinal tract. To summarize, 3.2 g of pepsin and 7 mL of hydrochloric acid were added to sufficient water, completely dissolved, and then the mixture was let to settle to form SGJ ($\text{pH} = 1.2$). About 6.8 g potassium dihydrogen phosphate, 10.0 g trypsin, and 77 mL 0.2 mol/L sodium hydroxide solution were added all at once to water to produce SIF ($\text{pH} = 7.4$). Subsequently, the florfenicol hydrogels were initially placed in SGJ (4 h) and subsequently in SIF (8 h) to assess their pH-responsive performance. Simultaneously, as the control, florfenicol hydrogels were always placed in SGJ (12 h) and SIF (12 h), respectively. At different time points (5, 10, 30, 60, 120, 180, 240, 360, 480 and 720 minutes), the differences in morphology of florfenicol hydrogels in different environments (SGJ and SIF) were observed. Meanwhile, the cumulative curve was plotted according to the cumulative-release percentage. Briefly, the florfenicol hydrogels were placed in a dialysis bag (MW: 3500) and then in 500 mL different environments (SGJ and SIF) at $37 \pm 0.5^\circ\text{C}$. At 0.5, 1, 2, 3, 4, 6, 8, 12, 24, 36, and 48 h, 1 mL of the dialysates were taken out, and the florfenicol concentrations were determined.

Antibacterial Activity of Florfenicol Hydrogels

Determination of Inhibition Zones

The inhibitory zones of florfenicol hydrogels and florfenicol against *E. coli* ATCC 25922 and *E. coli* isolates were estimated. To summarize, 15 mL of agar medium was placed into an aseptic plate, and when the agar solidified, an additional 5 mL of agar medium was added. This agar medium included 0.1 mL of bacterial fluid, which contained 1×10^6 CFU/mL *E. coli*. After the agar had set, the holes were made using a straw that was adequate. Then, 50 μL florfenicol hydrogels and florfenicol active pharmaceutical ingredients (10 $\mu\text{g}/\text{mL}$ florfenicol) were introduced. Physiological saline was used as a control. The strain of *E. coli* was incubated for 24 hours at 37°C in an incubator with 5% CO_2 , after which the size of the inhibitory zones was measured and noted.

Determination of the Minimum Inhibitory Concentration (MIC)

The MICs of florfenicol hydrogels and florfenicol active pharmaceutical ingredients against *E. coli* ATCC 25922 and *E. coli* isolates were determined using the broth macrodilution method. In summary, florfenicol hydrogels and florfenicol active pharmaceutical ingredients were produced in TSB at varying doses (128, 64, 32, 16, 8, 4, 2, 1, 0.5, 0.25, 1.25, 0.625, and 0.3125 µg/mL). Physiological saline was used as a control. On the other side, 1×10^6 CFU/mL was the concentration of *E. coli*. After 24 hours of culture, the lowest drug concentration that noticeably slowed down growth was the MICs. Every outcome was computed three times.

Live/Dead Bacterial Staining Analysis Using Fluorescent Microscope

In this study, *E. coli* ATCC 25922 and *E. coli* isolates (1×10^6 CFU/mL) were mixed with florfenicol hydrogels and florfenicol active pharmaceutical ingredients at varied doses “0×MIC, 1/2×MIC, 1×MIC, and 2×MIC”. Physiological saline was used as control. A live/dead fluorescent bacterial viability kit was applied to each sample after a 2-h incubation period. Eventually, 5 µL of bacterial solution that was placed on the slide was examined using a fluorescent microscope “(TS2R-FL, Japan)”.

Morphological Analysis Using SEM

In this work, SEM was used to observe *E. coli* ATCC 25922 or *E. coli* isolates treated with florfenicol hydrogels and florfenicol active pharmaceutical ingredients, as well as physiological saline (the control group). In summary, *E. coli* ATCC 25922 or *E. coli* isolates (1×10^6 CFU/mL) was cultivated in triplicate on a cover glass at 37°C for 24 hours. After that, the bacteria were dried out and repaired. Briefly, the samples were fixed for 2 h at 4°C using 2.5% glutaraldehyde. The sample was then dried using ethanol concentrations of “30%, 50%, 70%, 90%, 95%, and 100%” for a total of 20 minutes after the surfaces were cleaned twice with PBS for 15 minutes each. Finally, after a critical point drying and gold sputter coating, every sample was observed by SEM.

In vitro Biosafety Studies of Florfenicol Hydrogels

The hemocompatibility of hydrogels containing florfenicol was evaluated. In brief, heparin sodium was used to treat blood that had been extracted from a healthy rabbit in order to avoid clotting. Following the extraction of the red blood cells (RBCs), the blood was centrifuged for 5 minutes at 4°C at 1500×g. The blood was then washed three times with physiological saline. Ultimately, RBCs were suspended in physiological saline to create a 2% RBC suspension (v/v). Upon isolation, the RBC suspension was immediately used. To summarize, a 2% RBC solution was treated with several doses of florfenicol hydrogels (1000, 500, 200, 100, 50, and 10 µg/mL). After giving the mixture a quick shake, it was incubated at 37°C for 2 hours. Ultrapure water and physiological saline solution were simultaneously regarded as positive and negative controls, respectively. Eventually, the absorbance of the released hemoglobin at 540 nm was measured by photometry and analysis of the supernatants. The hemolysis degree was estimated by the following equation: calculated by the percent of hemolysis (%) = “ $(Ab_s - Ab_0) / (Ab_{s100} - Ab_{s0}) \times 100\%$ ”, where Ab_s , Ab_{s0} , and Ab_{s100} are the absorbances of test samples, the suspension treated with physiological saline, and ultrapure water, respectively.

Statistical Analysis

For all experimental data points that were given as mean±SD, a one-way ANOVA analysis was performed using the SPSS 19.0 software. The *p*-value was considered statistically significant when it was less than 0.05.

Results and Discussion

Formula Optimization

Appearance is one of the simplest, most effective, and most direct means to evaluate the preparation of hydrogels. In this study, florfenicol was encapsulated in different concentrations of SA (15, 25, and 35 mg/mL) and Ca²⁺ solution (2.5, 5.0, and 7.5 mg/mL) through complexation to obtain florfenicol hydrogels. Subsequently, the florfenicol hydrogels with different formulas were placed in a bottle, and their gel properties were observed at 0°, 45°, 90°, and 180° to choose the

optimal formula. When the concentration of SA was 35 mg/mL and Ca^{2+} was 7.5 mg/mL, the florfenicol hydrogels showed excellent gel properties (Figure 1A). The amount and proportion of different excipients result in different LC and EE of the formulation. The larger the LC and EE, the more drugs are encapsulated in the formulation. When LC is at its maximum, the optimal amount and proportion of the nanogels are obtained.^{21,22} Since florfenicol has been reported to be a broad-spectrum antibiotic with the disadvantage of poor aqueous solubility, the drug's preferential localization within the polymer matrix, which is less hydrophilic than the external aqueous environment, may be the cause of the high drug loading and entrapment efficiency. The response surface approach makes it easier to investigate and model formulation obstacles and process parameters by calculating the relationship between the response surfaces that are created and the controllable input parameters. It accomplishes this by combining statistical and mathematical approaches.²³ Thirteen experimental runs with three repeated center points were required in order to provide an appropriate estimate of the prediction variance throughout the whole design space of the model. The trial design and results generated by the Design-Expert program are shown in Table 1. The results of the thirteen groups were displayed in Tables 2 and 3 after the analysis, along with the quadratic polynomial regression equation that connected the LC to three factors:

$$LC = +11.02 + 1.57 * A - 1.03 * B + 1.13 * AB$$

The quadratic polynomial regression equation between the EE and three factors was:

$$EE = 64.95 + 24.52 * A - 5.70 * B + 3.55 * AB$$

The differences between the various treatments of the EE and LC models were extremely significant ($p < 0.0001$), indicating that the residuals were entirely the product of random errors, even though the lack of fit was not significant ($p > 0.05$). Reflecting the range of response values, the regression equation coefficients R^2 , adjusted R^2 , and pre- R^2 were all more than 0.93. More importantly, $|\text{adjusted } R^2 - \text{pre-}R^2| < 0.2$, demonstrating that both prediction models were reliable. Three-dimensional response surface images were generated based on the above data (Figure 1B-C). The optimized florfenicol hydrogels, according to Design-Expert software, were 32 mg/mL SA and 3.9 mg/mL CaCl_2 . The LC and EE predicted by the software were 12.2% and 83.9%, respectively (Figure 1D). The desirability was 93.3%. Subsequently, the optimal formulation was verified by producing florfenicol hydrogels with 32 mg/mL SA and 4.0 mg/mL CaCl_2 . The LC and EE of the prepared florfenicol hydrogels were $13.5\% \pm 0.70\%$ and $90.0\% \pm 1.1\%$, respectively. Thus, the optimal preparation method for the florfenicol hydrogels designed by the box-behnken response surface technique was accurate and reliable.

Characterization of Optimal Florfenicol Hydrogels

The appearance, TEM, SEM, resolvability, and FTIR spectrum of optimal florfenicol hydrogels are shown in Figure 2. The appearance of florfenicol hydrogels in the bottle was light yellow and showed excellent gel properties at 0° , 45° , 90° , and 180° (Figure 2A). A TEM analysis revealed that the florfenicol hydrogels had been properly synthesized, as evidenced by their spherical shape, smooth surface, and excellent particle size distributions. EDS of florfenicol hydrogels indicated that C, N, O, S, Na, and Ca were uniformly distributed in the florfenicol hydrogels. Thus, florfenicol hydrogels have been successfully prepared through complexation force (Figure 2B). The mean size, ZP, and PDI of florfenicol hydrogels were 531.9 ± 12.6 nm (Figure 2C), -33.0 ± 0.8 mV, and 0.24 ± 0.11 , respectively. This demonstrated the homogeneous dispersion and nanoscale nature of the florfenicol hydrogels. This indicates that medications have an easy time penetrating bacterial cell membranes and killing germs. SEM of freeze-dried florfenicol hydrogels showed a three-dimensional network structure (Figure 2D). In addition, the freeze-dried florfenicol hydrogels were easily dissolved in ultrapure water (Figure 2E), which improved the water solubility of florfenicol. The FTIR spectrum of SA, florfenicol, and florfenicol hydrogels is shown in Figure 2F. FTIR spectroscopy was used to study drug-hydrogel interactions. Physicochemical interactions, such as hydrogen bonding between medicines and SA or Ca^{2+} , can cause frequency changes or splitting in absorption peaks. The distinctive peaks for florfenicol at 3446, 3326, 1686, and 1542 cm^{-1} vanished from the spectrum of florfenicol hydrogels, and new characteristic peaks (1692 and 1532 cm^{-1}) were visible instead, which may be attributed to the complexation force between SA and Ca^{2+} . Thus, the preparation of the florfenicol hydrogels was successful. To determine the rheological characteristics of florfenicol hydrogels, a rheometer was used to

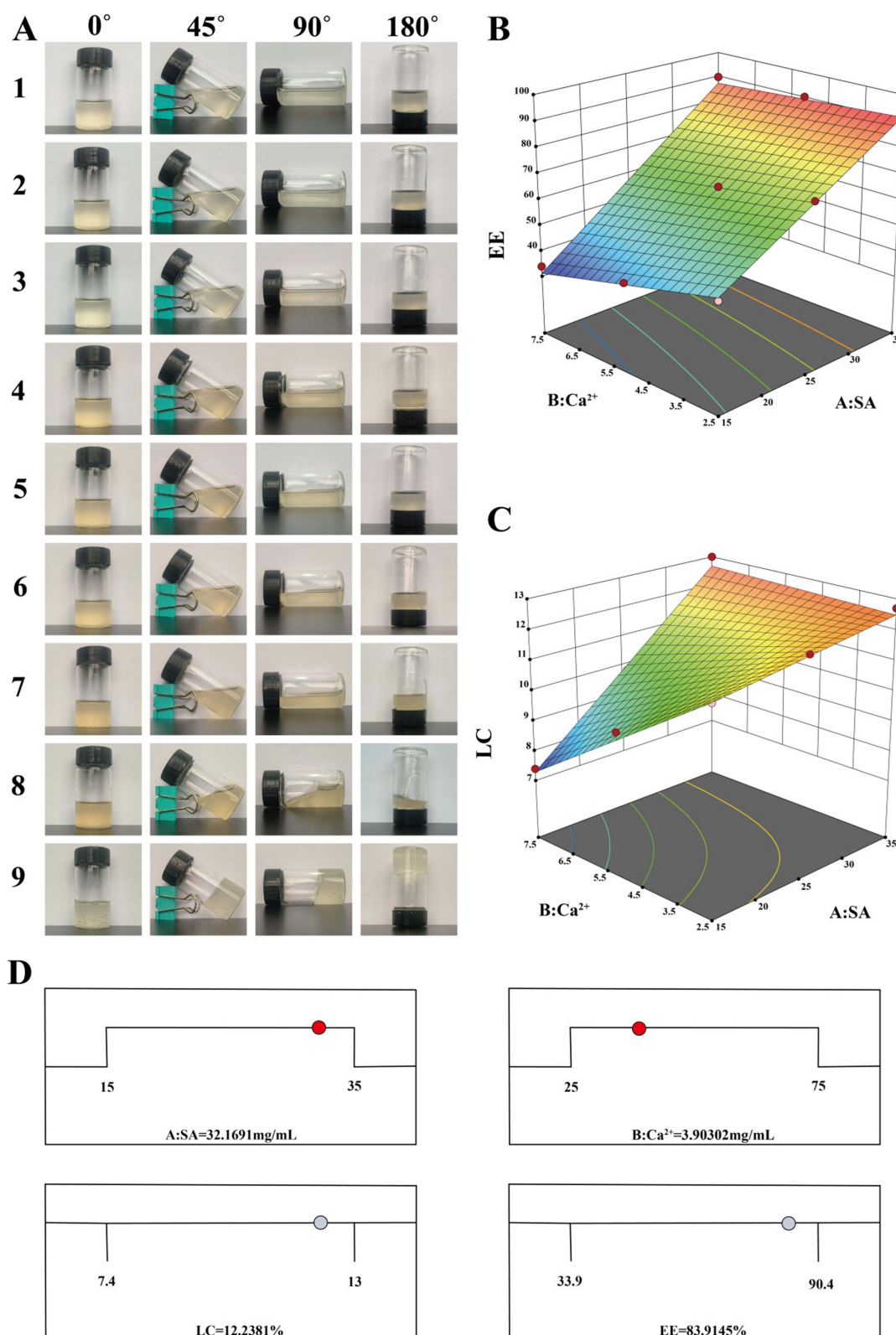


Figure 1 Optimization of florfenicol hydrogels formulations. **(A)**: Appearance of florfenicol hydrogels with different formulas at 0°, 45°, 90°, and 180°. Three-dimensional arrangement for response surface images of the different concentrations of SA, and CaCl₂ to LC **(B)** and EE **(C)**. **(D)** The optimal formula predicted by Design-Expert software.

Table 2 ANOVA of LC Model

Source	Sum of Squares	df	Mean Square	F-value	P-value
Model	26.20	3	8.73	217.64	<0.0001
A-SA	14.73	1	14.73	367.06	<0.0001
B-Ca ²⁺	6.41	1	6.41	159.68	<0.0001
AB	5.06	1	5.06	126.18	<0.0001
Residual	0.3611	9	0.0401		
Lack of Fit	0.3611	5	0.0722		
Pure Error	0.0000	4	0.0000		
Cor Total	26.56	12			
R ²	0.9864				
Adj-R ²	0.9819				
Pre-R ²	0.9354				
Adeq precision	48.4514				
CV%	1.82				
Mean	11.02				
Std.Dev.	0.2003				

Table 3 ANOVA of EE Model

Source	Sum of Squares	df	Mean Square	F-value	P-value
Model	3851.75	3	1283.92	171.54	<0.0001
A-SA	3606.40	1	3606.40	481.85	<0.0001
B-Ca ²⁺	194.94	1	194.94	26.05	0.0006
AB	50.41	1	50.41	6.74	0.0290
Residual	67.36	9	7.48		
Lack of Fit	67.36	5	13.47		
Pure Error	0.0000	4	0.0000		
Cor Total	3919.11	12			
R ²	0.9828				
Adj-R ²	0.9771				
Pre-R ²	0.9406				
Adeq precision	39.8232				
CV%	4.21				
Mean	64.95				
Std.Dev	2.74				

measure the storage modulus (G') and loss modulus (G'') of the materials over time at a given frequency (1 rad/s). The formation of the florfenicol hydrogels in a matter of seconds made it challenging to identify the junction of G' and G'' immediately. As shown in Figure 2G, G' of the florfenicol hydrogels was dominating across the complete period, suggesting that they were stable. After florfenicol hydrogels were applied to the bent fingers, florfenicol hydrogels will closely adhere to the fingers at the knuckle (0°, 45°, 90°, and 180°), which indicated that florfenicol hydrogels had excellent adhesion (Figure 2H).

Stability Evaluation of Florfenicol Hydrogels

In order to investigate the stability of florfenicol hydrogels, influencing-factor experiments, which included high temperature (40°C), high humidity (90%±5%), and intense light (4500±500 L×), were carried out by using their

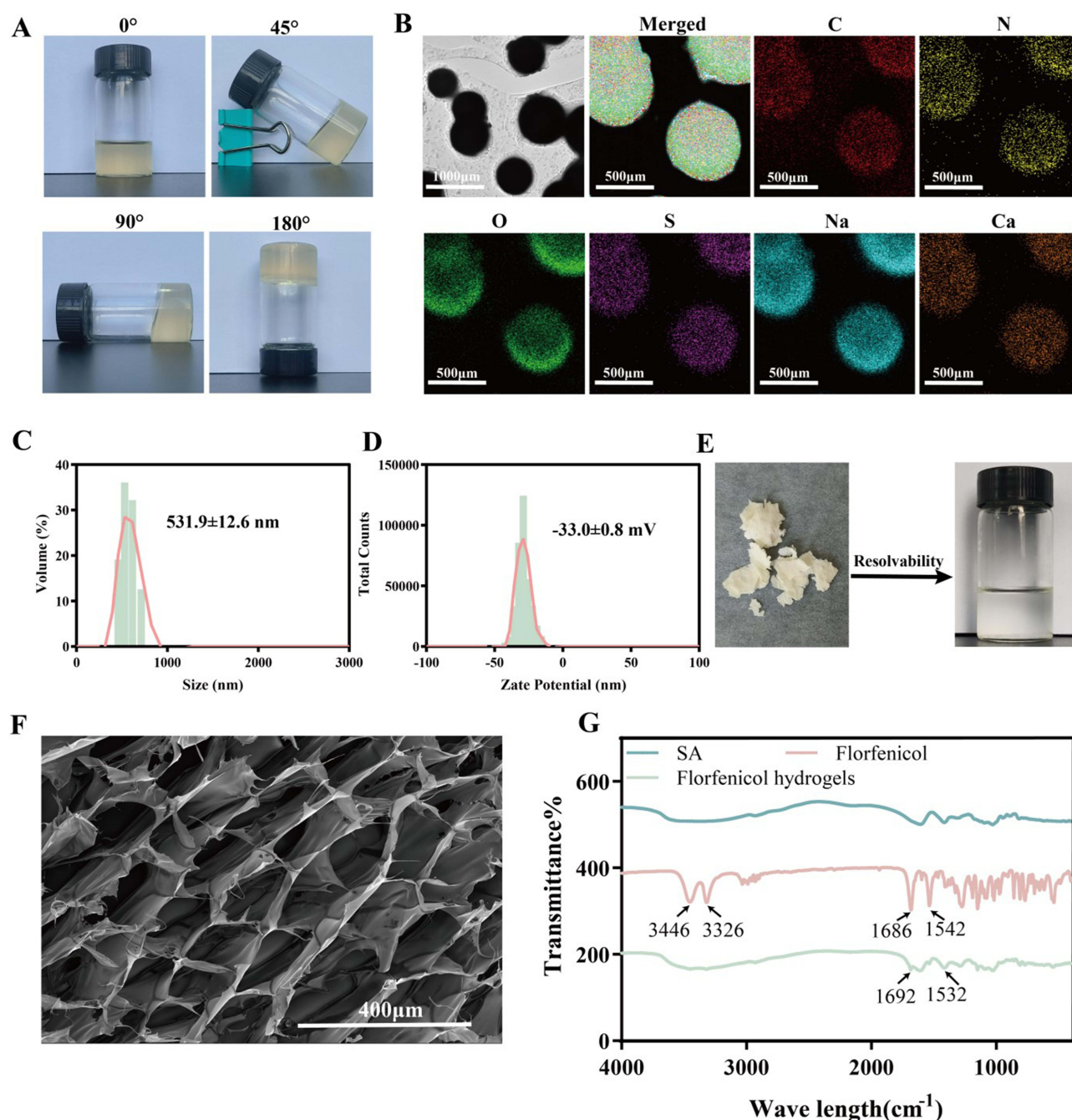


Figure 2 Characteristics of florfenicol hydrogels. Appearance (**A**), TEM (**B**); Size distribution (**C**); Zeta potential (**D**); SEM (**E**); resolubility (**F**); FTIR (**G**).

appearance, EE, LC, size, ZP, PDI, and FTIR spectrophotometer as an evaluation indicator. There were no significant differences in appearance (always light yellow with excellent gel properties at 0°, 45°, 90°, and 180°) (**Figure 3A**), EE (about 90%) (**Figure 3B**), LC (about 13%) (**Figure 3C**), size (about 530 nm) (**Figure 3D**), ZP (about -33 mV) (**Figure 3E**), PDI (about 0.2) (**Figure 3F**), and FTIR spectrophotometer (**Figure 3G-I**) on the fifth and tenth days. It is suggested that the prepared florfenicol hydrogels hold satisfactory stability.

pH-Responsive Performances of Florfenicol Hydrogels

In this study, the pH-responsive performance of florfenicol hydrogels in the gastrointestinal tract was systematically evaluated (**Figure 4A**). The florfenicol hydrogels had no obvious structural decomposition in SGJ (pH=1.2) for

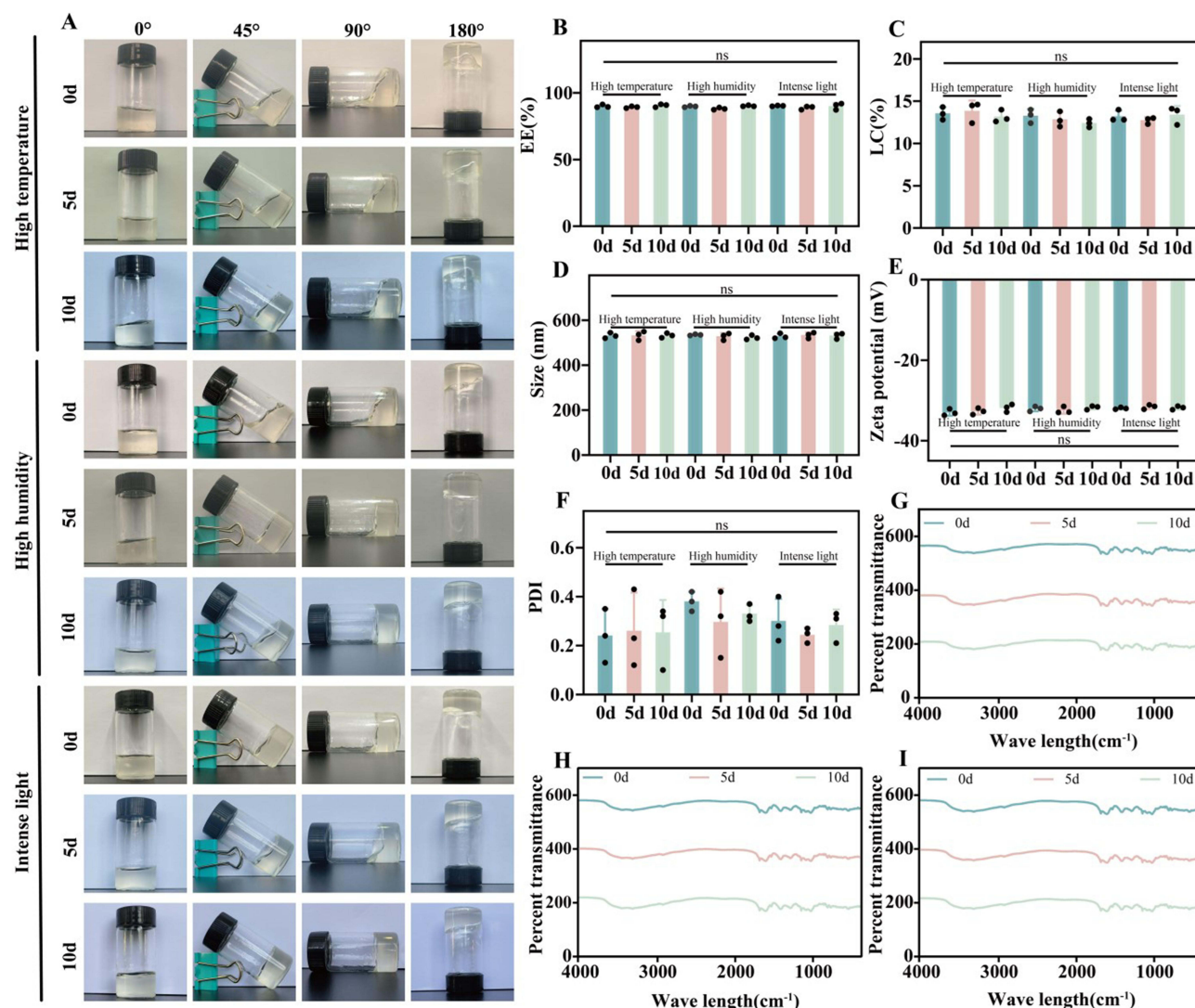


Figure 3 The influence factors test (high temperature, high humidity, and intense light) of florfenicol hydrogels. Appearance of florfenicol hydrogels at 0°, 45°, 90° and 180° (A); EE (B); LC (C); size (D); ZP (E); PDI (F); FTIR spectrophotometer (G: high temperature, (H) high humidity, (I) intense light).

720 minutes and were highly stable (Figure 4B). At 720 minutes, $24.5\% \pm 3.7\%$ of the florfenicol was released from the florfenicol hydrogels in SGJ (Figure 4C). The structure of the hydrogel began to be decomposed after 5 minutes in SIF, and this decomposition has been continuing (Figure 4B). At 720 minutes, the structure of the hydrogel was decomposed most obviously. At 720 minutes, $93.0\% \pm 3.4\%$ of the florfenicol was released from the florfenicol hydrogels in SGJ (Figure 4D). The florfenicol hydrogels were put in SGJ for 4 hours, and then placed in SIF for 8 hours due to the gastric emptying time is about 4 hours. The overall structure of the florfenicol hydrogels in SGJ was not significantly decomposed within 4 hours, and $18.4\% \pm 2.2\%$ of the florfenicol were released. Subsequently, the overall structure of the florfenicol hydrogels underwent significant decomposition in SIF (Figure 4B). With the decomposition of the structure of florfenicol hydrogels, the encapsulated florfenicol was also released, thus achieving the targeted-release effect. At 720 minutes, $96.1\% \pm 3.2\%$ of the florfenicol was released from florfenicol (Figure 4E). These findings contribute to the preparation of florfenicol hydrogels for the treatment of intestinal infections, including *E. coli*, *Salmonella*, and *Lawsonia intracellularis* infections. In this study, the swelling is limited in gastric conditions due to the protonated carboxyl groups, resulting in only a tiny amount being released. For the time being, the primary cause of florfenicol release will be its dispersion through the insoluble matrix. However, due to strong chain repulsion and carboxylate ionization, the matrix is structurally more relaxed in intestinal circumstances.²⁴ As a result, polymer chains

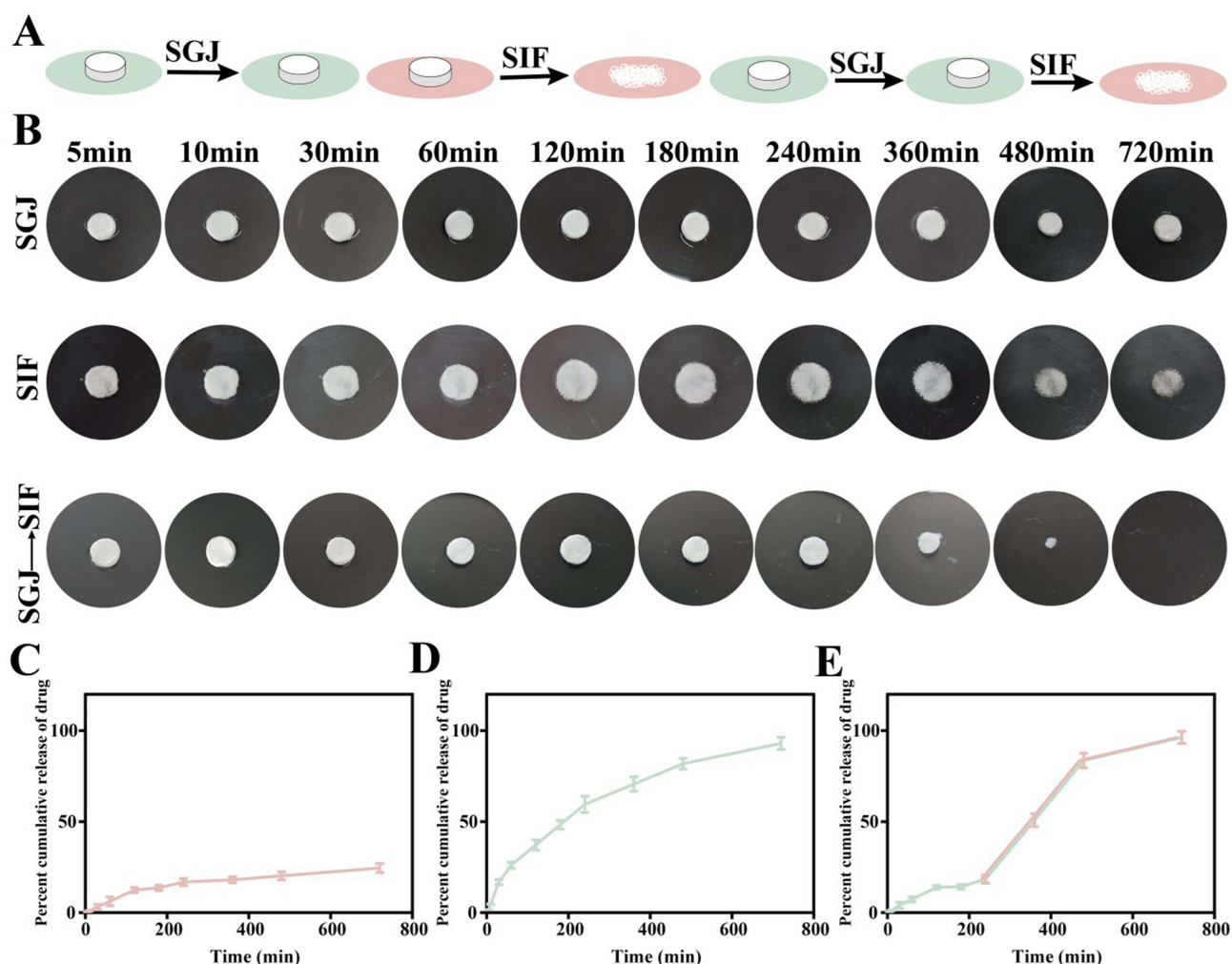


Figure 4 Effectively avoiding SGJ degradation and enhancing targeted and slow release of florfenicol hydrogels in SIF (n= 3). **(A):** Morphology change of florfenicol hydrogels at different time points in SGJ and SIF **(B)**. In vitro release of florfenicol hydrogels in SGJ (720 min) **(C)**, SIF (720 minutes) **(D)**, and in SGJ (240 minutes) and SIF (720 minutes) **(E)**.

become more flexible, and the mean pore size increases, releasing most of the medication. Because of its high lipid solubility, florfenicol was quickly absorbed into the intestinal tract. The results were consistent with previously published data, which showed that the chitosan alginate hydrogels suppressed the release of the drug in simulated gastric fluid “below 10% for 2 h” and enhanced the release in simulated intestinal fluids “up to 84% for 24 h”.²⁵ In addition, it should be noted that florfenicol hydrogels can resist the gastric pH due to their absorption from the intestinal epithelium, but other oral florfenicol formulations do have the same pattern of passing through the stomach and being absorbed from the intestine.

In vitro Antibacterial Activity Studies of Florfenicol Hydrogels

The in vitro antibacterial activity of florfenicol and florfenicol hydrogels against *E. coli* ATCC 25922 and *E. coli* isolates are shown in Figure 5. The inhibition zones of florfenicol and florfenicol hydrogels were 2.43 ± 0.04 and 2.54 ± 0.14 cm for *E. coli* ATCC 25922 (Fig. 5A), and 1.88 ± 0.12 and 2.76 ± 0.11 cm for *E. coli* isolates (Figure 5B), respectively. The MICs of florfenicol and florfenicol hydrogels were 4 and 1 $\mu\text{g/mL}$ for *E. coli* ATCC 25922, and 4 and 2 $\mu\text{g/mL}$ for *E. coli* isolates respectively. Therefore, compared to florfenicol, florfenicol hydrogels demonstrated greater antibacterial activity against *E. coli* ATCC 25922 and *E. coli* isolates. In addition, the mixture of *E. coli* ATCC 25922 or *E. coli* isolates with florfenicol and florfenicol hydrogels was treated using a live/dead bacterial staining kit. The findings indicated that florfenicol hydrogels exhibited more bactericidal action, as shown by the rise in dead bacteria (colored red) and reduction

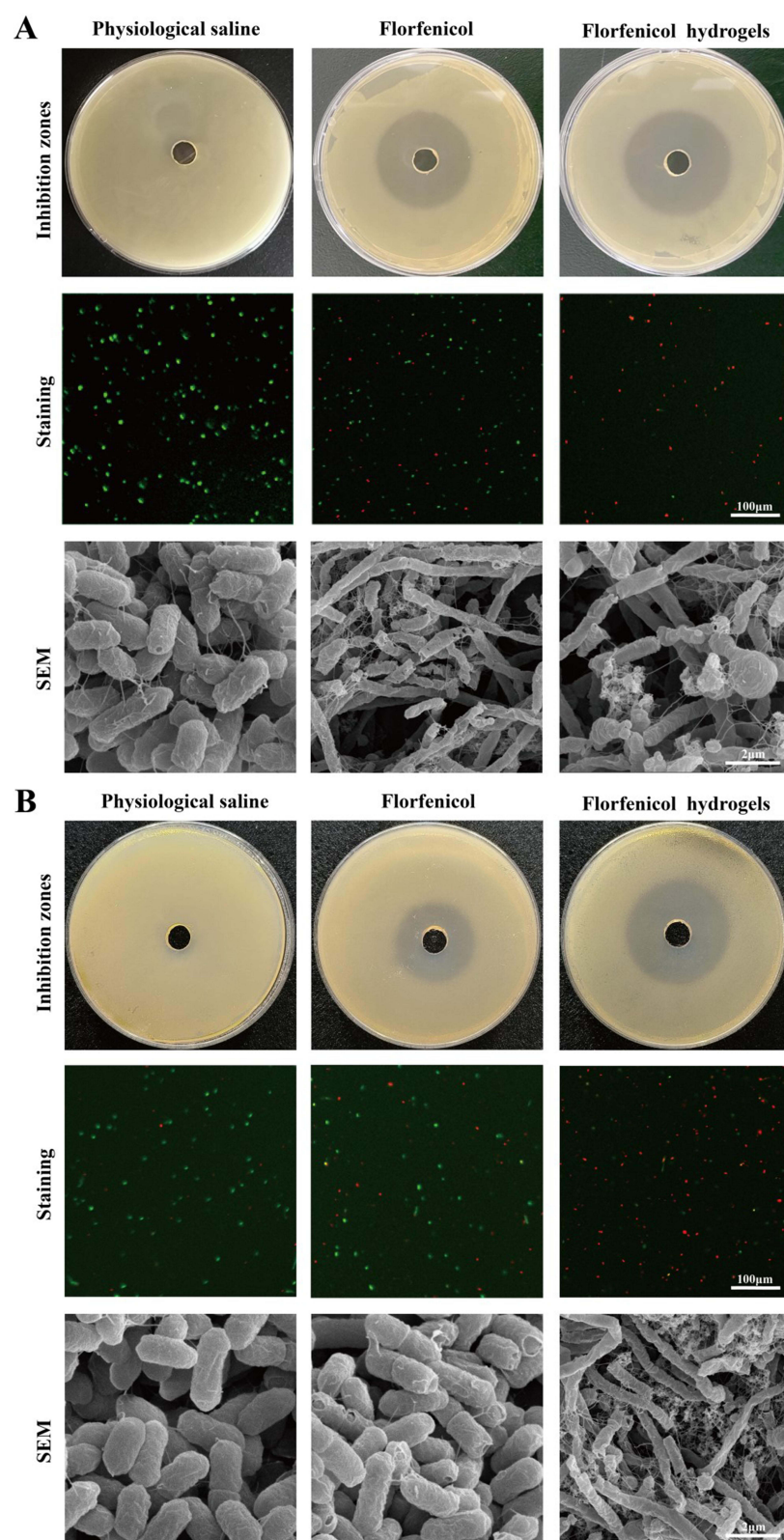


Figure 5 The antibacterial effect of florfenicol and florfenicol hydrogels against *E. coli* ATCC 25922 (A) and *E. coli* isolates (B).

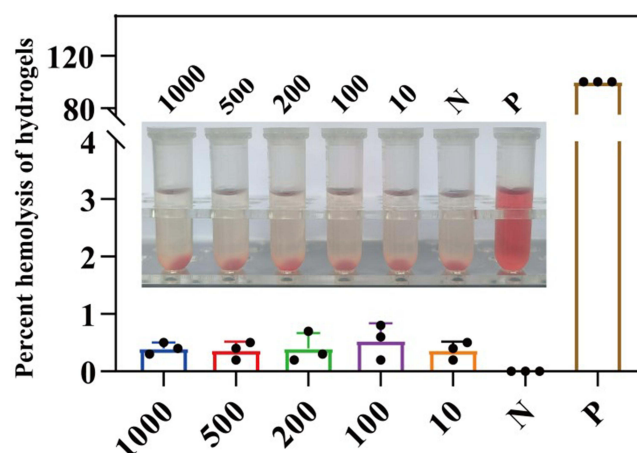


Figure 6 In vitro biosafety studies.

in live bacteria (colored green) (Figure 5A and B). After the *E. coli* ATCC 25922 was treated with florfenicol, SEM showed that *E. coli* ATCC 25922 had become thin and long, and some holes appeared, indicating a change in its morphology. Especially after being treated with florfenicol hydrogels, *E. coli* ATCC 25922 not only became thin and long, with some holes appearing, but also became spherical (Figure 5A). After the *E. coli* isolates were treated with florfenicol, the bacterial surface suffered a large amount of damage, which may have been caused by florfenicol leading to the rupture of the bacterial cell wall. After the *E. coli* isolates were treated with florfenicol hydrogels, bacteria also become thinner and longer, and their surface was more severely damaged, which may be caused by the rupture of bacterial cell walls and membranes after using florfenicol hydrogels, killing a large number of bacteria (Figure 5B). These results indicated that the florfenicol hydrogels had caused significant morphological changes in bacteria. The produced nanocomposite is more efficient against *Salmonella Typhimurium*, *Staphylococcus aureus*, and *E. coli* than its natural florfenicol, according to the data. The ability of the nanocomposite to target the respiratory chain and the microorganism's ability to divide its cells, ultimately leading to cell death, were cited to have the best antibacterial action. Furthermore, the created polycationic florfenicol nanocomposite might interact with the negatively charged bacterial surface with a high affinity. Furthermore, their vast surface area allowed for their tight absorption onto the bacterial surface, which disrupted the bacterial membrane and led to leakage of intracellular compounds and caused bacterial death.

In vitro Biosafety Studies

Hemolysis studies were one of the most important factors in evaluating the safety of drug formulations. Hydrogel needs to have long-term stability and minimal interaction with circulatory components in order to be used for medication delivery. Each material can be classified into one of three categories, as per the "American Society for Testing and Materials (ASTM F 756–00, 2000)": "hemolytic (defined as hemolysis over 5%), somewhat hemolytic (defined as between 2% and 5%), or non-hemolytic (defined as below 2%)".²⁶ In this study, compared with the negative control and the positive control, different concentrations of florfenicol hydrogels (1000, 500, 200, 100, 50, and 10 µg/mL) did not show hemolysis (Figure 6). Furthermore, the hemolysis rates of different concentrations (1000, 500, 200, 100, 50, and 10 µg/mL) of florfenicol hydrogels were $0.40 \pm 0.10\%$, $0.37 \pm 0.15\%$, $0.40 \pm 0.26\%$, $0.53 \pm 0.30\%$, and $0.37 \pm 0.15\%$, respectively. In this regard, each group's hemolysis rate was less than 5%, demonstrating their outstanding biocompatibility.

Conclusions

In this study, the florfenicol hydrogels were successfully prepared through complexation. The prepared florfenicol hydrogels can achieve the effect of slow release at the site of intestinal infection, thereby enhancing the antibacterial activity of florfenicol against intestinal bacteria. Although the preparation of the florfenicol hydrogels is simple,

florfenicol hydrogels had excellent physicochemical properties, such as nano-size, obvious pH-responsiveness, high stability, and can improve the antibacterial activity of the prepared hydrogels. However, clinical therapeutic experiments were not added to this study; thus, we will conduct detailed therapeutic experiments in the future work to demonstrate the advantages of hydrogels. Overall, the florfenicol hydrogels in this study will have slow antibacterial activity against intestinal bacteria in veterinary clinics.

Data Sharing Statement

The data used to support the findings of this study are available from the corresponding author upon request.

Acknowledgments

The authors acknowledge the assistance of Instrumental Analysis Center of Tarim University (Zhiqiang Zhou, Lijun Wang, Beibei Sun, and Ning Du). The authors would like to thank Wang Wenqian from Shiyanjia Lab (www.shiyanjia.com) for the FTIR analysis.

Funding

The article is financially supported by the National Natural Science Foundation of China (32460904), the second group of Tianshan Talent Training Program: Youth Support Talent Project (2023TSYCQNTJ0033), Natural Science Support Program of Xinjiang Production and Construction Corps (2024DA029).

Disclosure

The authors declare no conflicts of interest in this work.

References

1. Trif E, Cerbu C, Olah D, et al. Old antibiotics can learn new ways: a systematic review of florfenicol use in veterinary medicine and future perspectives using nanotechnology. *Animals*. 2023;13(10):1695.
2. Fang Y, Li S, Ye L, et al. Increased bioaffinity and anti-inflammatory activity of florfenicol nanocrystals by wet grinding method. *J Microencapsul*. 2020;37(2):109–120.
3. Somogyi Z, Mag P, Simon R, et al. Pharmacokinetics and pharmacodynamics of florfenicol in plasma and synovial fluid of pigs at a dose of 30 mg/kgbw following intramuscular administration. *Antibiotics*. 2023;12(4):758.
4. Abonashy SG, Hassan HAFM, Shalaby MA, Fouad AG, Mobarez E, El-Banna HA. Formulation, pharmacokinetics, and antibacterial activity of florfenicol-loaded niosome. *Drug Deliv Transl Res*. 2024;14(4):1077–1092. doi:10.1007/s13346-023-01459-9
5. Li Z, Yang YJ, Qin Z, et al. Florfenicol-polyarginine conjugates exhibit promising antibacterial activity against resistant strains. *Front Chem*. 2022;10:921091.
6. Ueda Y, Suenaga I. In vitro antibacterial activity of florfenicol against *Actinobacillus pleuropneumoniae*. *J Vet Med Sci*. 1995;57(2):363–364. doi:10.1292/jvms.57.363
7. Luo W, Meng K, Zhao Y, et al. Guar gum modified tilmicocin-loaded sodium alginate/gelatin composite nanogels for effective therapy of porcine proliferative enteritis caused by *Lawsonia intracellularis*. *Int J Biol Macromol*. 2023;242(Pt 3):125084. doi:10.1016/j.ijbiomac.2023.125084
8. Gutierrez L, Guzman-Flores A, Monroy-Barreto M, Ocampo L, Sumano H. Oral pharmacokinetics of a pharmaceutical preparation of florfenicol in broiler chickens. *Front Vet Sci*. 2023;10:1208221. doi:10.3389/fvets.2023.1208221
9. Zhu W, Liu YQ, Liu P, Cao J, Shen AG, Chu PK. Blood-glucose-depleting hydrogel dressing as an activatable photothermal/chemodynamic antibacterial agent for healing diabetic wounds. *ACS Appl Mater Interfaces*. 2023;15(20):24162–24174. doi:10.1021/acsami.3c03786
10. Xue C, Xu X, Zhang L, et al. Self-healing/pH-responsive/inherently antibacterial polysaccharide-based hydrogel for a photothermal strengthened wound dressing. *Colloids Surf B Biointerfaces*. 2022;218:112738. doi:10.1016/j.colsurfb.2022.112738
11. Chen T, Chen Y, Rehman HU, et al. Ultratough, self-healing, and tissue-adhesive hydrogel for wound dressing. *ACS Appl Mater Interfaces*. 2018;10(39):33523–33531. doi:10.1021/acsami.8b10064
12. Kapusta O, Jarosz A, Stadnik K, Giannakoudakis DA, Barczyński B, Barczak M. Antimicrobial natural hydrogels in biomedicine: properties, applications, and challenges-a concise review. *Int J Mol Sci*. 2023;24(3):2191. doi:10.3390/ijms24032191
13. Luo W, Ju M, Liu J, Algharib SA, Dawood AS, Xie S. Intelligent-responsive enrofloxacin-loaded chitosan oligosaccharide-sodium alginate composite core-shell nanogels for on-demand release in the intestine. *Animals*. 2022;12(19):2701. doi:10.3390/ani12192701
14. Li C, Yuan L, Zhang X, et al. Core-shell nanosystems designed for effective oral delivery of polypeptide drugs. *J Control Release*. 2022;352:540–555. doi:10.1016/j.jconrel.2022.10.031
15. Xu J, Cao L, Suo Y, et al. Chitosan-microcapsulated insulin alleviates mesenteric microcirculation dysfunction via modulating COX-2 and VCAM-1 expression in rats with diabetes mellitus. *Int J Nanomed*. 2018;13:6829–6837. doi:10.2147/IJN.S174030
16. Zhang Y, Kang R, Zhang X, et al. A programmable oral bacterial hydrogel for controllable production and release of nanovaccine for tumor immunotherapy. *Biomaterials*. 2023;299:122147. doi:10.1016/j.biomaterials.2023.122147
17. Qin B, Wu S, Dong H, et al. Accelerated healing of infected diabetic wounds by a dual-layered adhesive film cored with microsphere-loaded hydrogel composite dressing. *ACS Appl Mater Interfaces*. 2023;15(28):33207–33222. doi:10.1021/acsami.2c22650

18. Ceylan O, Karakus H, Cicek H. Design and in vitro antibiofilm activity of propolis diffusion-controlled biopolymers. *Biotechnol Appl Biochem*. 2021;68(4):789–800. doi:10.1002/bab.1991
19. Wu P, He RH, Fang Y, et al. The study of double-network carboxymethyl chitosan/sodium alginate based cryogels for rapid hemostasis in noncompressible hemorrhage. *Int J Biol Macromol*. 2024;266(Pt 1):131399. doi:10.1016/j.ijbiomac.2024.131399
20. Zhou K, Wang X, Chen D, et al. Enhanced treatment effects of tilmicosin against staphylococcus aureus cow mastitis by self-assembly sodium alginate-chitosan nanogel. *Pharmaceutics*. 2019;11(10):524. doi:10.3390/pharmaceutics11100524
21. Algharib SA, Dawood A, Zhou K, et al. Designing, structural determination and biological effects of rifaximin loaded chitosan-carboxymethyl chitosan nanogel. *Carbohydr Polym*. 2020;248:116782. doi:10.1016/j.carbpol.2020.116782
22. Zhang Y, Zuo R, Song X, et al. Optimization of maduramicin ammonium-loaded nanostructured lipid carriers using box-behnken design for enhanced anticoccidial effect against Eimeria tenella in broiler chickens. *Pharmaceutics*. 2022;14(7):1330. doi:10.3390/pharmaceutics14071330
23. Asfour MH, Kassem AA, Salama A. Topical nanostructured lipid carriers/inorganic sunscreen combination for alleviation of all-trans retinoic acid-induced photosensitivity: box-Behnken design optimization, in vitro and in vivo evaluation. *Eur J Pharm Sci*. 2019;134:219–232. doi:10.1016/j.ejps.2019.04.019
24. Luo W, Liu J, Zhang M, et al. Florfenicol core-shell composite nanogels as oral administration for efficient treatment of bacterial enteritis. *Int J Pharm*. 2024;662:124499. doi:10.1016/j.ijpharm.2024.124499
25. Hoang HT, Vu TT, Karthika V, et al. Dual cross-linked chitosan/alginate hydrogels prepared by Nb-Tz ‘click’ reaction for pH responsive drug delivery. *Carbohydr Polym*. 2022;288:119389. doi:10.1016/j.carbpol.2022.119389
26. Luo W, Jiang Y, Liu J, Ju M, Algharib SA, Dawood AS. On-demand release of enrofloxacin-loaded chitosan oligosaccharide-oxidized hyaluronic acid composite nanogels for infected wound healing. *Int J Biol Macromol*. 2023;253(Pt 6):127248. doi:10.1016/j.ijbiomac.2023.127248

International Journal of Nanomedicine

Publish your work in this journal

The International Journal of Nanomedicine is an international, peer-reviewed journal focusing on the application of nanotechnology in diagnostics, therapeutics, and drug delivery systems throughout the biomedical field. This journal is indexed on PubMed Central, MedLine, CAS, SciSearch®, Current Contents®/Clinical Medicine, Journal Citation Reports/Science Edition, EMBase, Scopus and the Elsevier Bibliographic databases. The manuscript management system is completely online and includes a very quick and fair peer-review system, which is all easy to use. Visit <http://www.dovepress.com/testimonials.php> to read real quotes from published authors.

Submit your manuscript here: <https://www.dovepress.com/international-journal-of-nanomedicine-journal>

Dovepress
Taylor & Francis Group